YOKOK8NQTVBCNP7VCE

T.C.
YÜKSEKÖĞRETİM KURULU BAŞKANLIĞI
ANKARA

05.03.2024

OKUL TANIMA BELGESİ

T.C. Kimlik No	: 22520560338
Adı Soyadı	: İLKAY DEMİR
Ülke	: TUNUS
Üniversite	: Faculté des Sciences de Sfax
Durumu	: Kurulumuzda mevcut uluslararası listelerde yer almaktadır.

Açıklama

Yurtdışındaki yükseköğretim kurumlarından örgün eğitim yoluyla alınan diplomaların denklik işlemi, 2547 sayılı Yükseköğretim Kanunu'nun 2880 sayılı kanunla değişik 7/p maddesi ile 05.12.2017 tarihli Resmi Gazete'de yayımlanan *"Yurtdışı Yükseköğretim Diplomaları Tanıma ve Denklik Yönetmeliği"* hükümleri uyarınca yapılmakta olup, söz konusu Yönetmelik yatay geçiş, dikey geçiş ve lisans tamamlama gibi kavramları kapsamamaktadır.
Yurtdışındaki yükseköğretim kurumlarından uzaktan öğretim yoluyla alınacak diplomalar ise söz konusu Yönetmeliğin 10. maddesi ve ilgili mevzuat çerçevesinde değerlendirilmektedir.
Öğrenim dili Türkçe olan yurt dışındaki yükseköğretim programlarından alınan diplomalar için yapılan başvurular Yönetmelik'in 7. madde, 6. fıkra, (ç) bendi *"Türkiye'nin taraf olduğu uluslararası anlaşmalarla öğrenim dilinin Türkçe olduğu belirlenen programlar veya Yükseköğretim Kurulunca tanınan yurtdışındaki Türkçe yükseköğretim programları dışında, yükseköğretim kurumlarının açtığı ve öğrenim dili Türkçe olan programlardan alınan diplomalar için yapılan başvurular reddedilir."* hükmü çerçevesinde karara bağlanacaktır.
Diploma denklik başvurusunda aranacak belgeler ile inceleme ve değerlendirme usul ve esasları Yurtdışı Yükseköğretim Diplomaları Tanıma ve Denklik Yönetmeliği'nde belirtilmiş olup; ilgili Yönetmelik ve detaylı bilgiye Yükseköğretim Kurulu web sayfasından ulaşılabilmektedir.
Yatay geçiş başvuruları, 08.02.2008 tarih ve 636/2732 sayılı yazımız ile "Yükseköğretim Kurumları Arasında Ön lisans ve Lisans Düzeyindeki Programlar Arasında Geçiş, Çift Anadal, Yan Dal ile Kurumlar Arası Kredi Transferi Yapılması Esaslarına İlişkin Yönetmelik" hükümlerine; lisansüstü eğitim başvuruları ise 26.09.2017 tarih ve 64528 sayılı yazı ile "Lisansüstü Eğitim ve Öğretim Yönetmeliği" hükümlerine uygun olarak, alınan dersler incelenmek suretiyle başvuru yapılan Üniversite tarafından değerlendirilmekte ve karara bağlanmaktadır.
2547 Sayılı Kanun'un 11 b/5 maddesi uyarınca yurtdışında yapılan doktora eğitimleri Üniversitelerarası Kurul tarafından değerlendirilmektedir. Yurtdışında yapılan doktora eğitiminin Türkiye'de yapılan doktoraya eşdeğer olup olmayacağı hususunda önceden herhangi bir görüş belirtmek mümkün olmadığı gibi, söz konusu eşdeğerlik, doktora tamamlandıktan sonra ilgili komisyon ve kurullar tarafından incelenmektedir.
Öte yandan diploma denklik başvuruları, ilgili Komisyon ve Kurullar tarafından münferiden değerlendirildiğinden yurt dışındaki yükseköğretim kurumlarından alınmış ön lisans, lisans ve yüksek lisans diplomalarının ülkemizdeki diplomalara eşdeğer olup olmayacağı hususunda önceden herhangi bir görüş belirtmek mümkün olmadığı gibi, eğitim alınan yükseköğretim kurumunun tanınırlığına ilişkin olarak Kurulumuzun yeni kararlar alma hakkı saklıdır.
Yurt dışında yükseköğrenim görmek isteyen öğrencilerin konuyla ilgili güncel gelişme ve kararları Kurulumuz internet adresinden takip etmeleri yararlarına olacaktır.
Bilgilerinizi rica ederim.

***BU BELGE DENKLİK BELGESİ YERİNE GEÇMEZ**

Search › Results for Altuntas I* (Auth... › Effect of substrate temperature on Raman study and optical properties of G...

Full text at publisher | Export | Add To Marked List

Effect of substrate temperature on Raman study and optical properties of GeO_x/Si thin films

By Baghdedi, D (Baghdedi, Dhouha) [1], [2], [3]; Hopoglu, H (Hopoglu, Hicret) [2], [3]; Demir, I (Demir, Ilkay) [3], [4]; Altuntas, I (Altuntas, Ismail) [3], [4]; Abdelmoula, N (Abdelmoula, Najmeddine) [1]; Tüzemen, ES (Tuzemen, Ebru Senadim) [2], [3]

Source JOURNAL OF THE AUSTRALIAN CERAMIC SOCIETY

DOI: 10.1007/s41779-023-00961-0

Early Access OCT 2023

Indexed 2023-11-26

Document Type Article; Early Access

Jump to ↓Enriched Cited References

Abstract

In this study, GeO(x)thin films were deposited onto Si substrates using the RF magnetron sputtering method. We looked at how the temperature of the substrate affected the Raman spectra and optical characteristics of GeOx thin films. X-ray diffraction was utilized to examine the crystal structure, and a scanning electron microscope was utilized to measure the thickness. In order to investigate the local structure and bonding characteristics, Raman spectroscopy was used. The refractive index, extinction coefficient, and dielectric parameters were calculated using spectroscopic ellipsometry for the 300-1100 nm spectral region. Refractive index and extinction coefficient spectral patterns were discovered by using a sample-air optical model to analyze the experimental ellipsometric data. Notably, a considerable rise in the refractive index was accompanied by a rise in substrate temperature.

Keywords

Author Keywords: GeOx; Raman spectrometry; RF; Optical study; Structural study

Keywords Plus: GERMANIUM DIOXIDE; PHOTOINDUCED PHENOMENA; GEO2; GROWTH

Author Information

Corresponding Address: Tuzemen, Ebru Senadim (corresponding author)

Sivas Cumhuriyet Univ, Dept Phys, TR-58140 Sivas, Turkiye

Journal information

JOURNAL OF THE AUSTRALIAN CERAMIC SOCIETY

Publisher name: SPRINGER

Journal Impact Factor ™

1.9 (2022) | 1.7 (Five Year)

JCR Category	Category Rank	Category Quartile
MATERIALS SCIENCE, CERAMICS *in SCIE edition*	13/29	Q2

Source: Journal Citation Reports 2022. Learn more

Journal Citation Indicator ™

0.43 (2022) | 0.41 (2021)

JCI Category	Category Rank	Category Quartile
MATERIALS SCIENCE, CERAMICS *in SCIE edition*	13/30	Q2

The Journal Citation Indicator is a measure of the average Category Normalized Citation Impact (CNCI) of citable items (articles and reviews) published by a journal over a recent three year period. It is used to help you evaluate journals based on other metrics besides the Journal Impact Factor (JIF).

Learn more

Interested in reviewing for this journal?

Add this journal to your reviewer interest list. Add Journal

Journal of the Australian Ceramic Society
https://doi.org/10.1007/s41779-023-00961-0

RESEARCH

Effect of substrate temperature on Raman study and optical properties of GeO_x/Si thin films

Dhouha Baghdedi[1,2,3] · Hicret Hopoğlu[2,3] · İlkay Demir[3,4] · İsmail Altuntaş[3,4] · Najmeddine Abdelmoula[1] · Ebru Şenadım Tüzemen[2,3]

Received: 20 March 2023 / Revised: 25 September 2023 / Accepted: 14 October 2023

Abstract

In this study, GeO_x thin films were deposited onto Si substrates using the RF magnetron sputtering method. We looked at how the temperature of the substrate affected the Raman spectra and optical characteristics of GeO_x thin films. X-ray diffraction was utilized to examine the crystal structure, and a scanning electron microscope was utilized to measure the thickness. In order to investigate the local structure and bonding characteristics, Raman spectroscopy was used. The refractive index, extinction coefficient, and dielectric parameters were calculated using spectroscopic ellipsometry for the 300–1100 nm spectral region. Refractive index and extinction coefficient spectral patterns were discovered by using a sample-air optical model to analyze the experimental ellipsometric data. Notably, a considerable rise in the refractive index was accompanied by a rise in substrate temperature.

Keywords GeO_x · Raman spectrometry · RF · Optical study · Structural study

Introduction

Nanotechnologies bring a strong potential for innovation and breakthroughs in wide areas. Because of their remarkable optical and electronic capabilities, nanoscale semiconductor oxide materials have recently gained more and more significance in manufacturing and engineering. Since the early 1900s, there has been a gradual revolution in the development of efficient semiconductor materials for electronic applications. As technology advances, the number of components in electrical gadgets increases. While many studies highlight the innovations promised by nanotechnology on general or specific scientific topics, very few address the path from novel properties to varied applications [1]. Highly doped GaN, as described by M. Rahman et al., are n-type large band gap semiconductors that are commonly used as transparent electrodes in solar cells, flat-panel displays, and light-emitting diode (LED) applications [2]. Md. F. Rahman and colleagues reported an innovative method for producing and analyzing transparent CdS thin layers that could be used for CdTe/CdS solar cells. They used the spin coating approach with thiol-amine solutions to effectively generate CdS thin films in air. Their findings indicate that CdS thin layers have a promising future for the creation of successful solution-processed CdTe/CdS photovoltaic cells [3]. Rashid et al. employed a simple solution-based approach to create VO_2 nanowires on a transparent substrate. Their SEM (scanning electron microscopy) study revealed the production of exceptionally dense and high-quality VO_2 nanowires at annealing temperature of 400 °C. The monoclinic VO_2 (B) phase was revealed by the patterns of X-ray diffraction (XRD) in the nanowire-embedded VO_2 thin layers. The optical band gap of these VO_2 thin films was found to have a value between 2.65 and 2.70 eV. Finally, the VO_2 nanowires were demonstrated to be capable of producing hydrogen via solar water splitting for use in a PEC system [4]. Following several studies, we have estimated that with the evolution of nanotechnology science, there is a significant interest in the

✉ Ebru Şenadım Tüzemen
esenadim@cumhuriyet.edu.tr

1 Laboratory of Multifunctional Materials and Applications (LaMMA), Faculty of Sciences of Sfax, University of Sfax, Sfax, Tunisia

2 Department of Physics, Sivas Cumhuriyet University, 58140 Sivas, Turkey

3 Nanophotonics Research and Application Center, Sivas Cumhuriyet University, 58140 Sivas, Turkey

4 Department of Nanotechnology Engineering, Sivas Cumhuriyet University, 58140 Sivas, Turkey

research and fabrication of both efficient and low-cost semiconductor thin film materials. One of the most significant goals is to employ nano-structured thin films efficiently in optical and optoelectronic applications. With this objective in mind, germanium dioxide (GeO_2) stands out as a versatile wide-band gap material with distinctive thermal, optical, and electrical characteristics [5]. These properties make GeO_2 a very interesting choice for a wide variety of applications, including vacuum technology, solar cells, catalysis, Li-ion batteries, and, most importantly, its critical role in optoelectronic devices as the core material for optical fibers [6–14]. In particular, we are interested in the contributions of nanotechnology to the development of optical, electronic, and optoelectronic devices and more specifically in the creation and characterization of GeO_2 thin films.

The fabrication of GeO_2 thin films was synthesized by physical evaporation [15], electro-spinning [16], laser ablation [17], and thermal evaporation [14]. The deposition process used has a considerable impact on the characteristics of thin films, and controlling growth parameters is critical for customizing them to be acceptable for a wide variety of applications [18]. In this study, GeO_2 films were produced depending on the substrate temperature by a radio frequency magnetron sputtering method. Following that, a study was carried out with the aim of analyzing both the optical and structural properties and how they relate to changes in substrate temperature.

Experimental details

Sample preparation

To explore the effect of substrate temperature on XRD, Raman, and optical results of GeO_x films, we employed RF magnetron sputtering using a NANOVAK NVTS-400-2TH2SP system. A 99.999% pure Ge target with a 50.8 mm diameter and 3.1 mm thickness was utilized. Commercial Ar gas with a purity of 99.99% was used as the sputtering gas, accounting for 92% of the gas mixture, while oxygen gas comprised the remaining 8%. The sputtering chamber was evacuated to get an ultimate pressure of 8.3×10^{-6} Torr. The working pressure, sputtering rotation, and RF power were set to 13×10^{-3} Torr, 10 rpm, and 60 W, respectively. The 240.60-nm-thick film used in this study was taken from the study by Baghdedi et al. [19]. This film was used to see the difference between substrate temperature and room temperature.

Characterization techniques

Several characterization techniques were used to evaluate the effect of substrate temperature on the properties of GeO_2 materials. The crystal structure of the studied samples was investigated using the X-ray diffraction technique. The thickness was measured using a scanning electron microscope (SEM). In terms of optical properties, we utilized an optical spectrophotometer (Cary 5000) covering the UV–Vis-NIR wavelength range from 200 to 1200 nm and spectroscopic ellipsometry (OPT-S9000) to examine the optical characteristics of the fabricated samples. We adopted a Raman spectrometer (LABRAM HRT 4600 h 800, LaMMA, Sfax, Tunisia) with a He + ion laser (= 532 nm) to record Raman spectra from 50 to 1000 cm^{-1} at room temperature (RT).

Results and discussion

X-ray diffraction (XRD) technique

The structural properties of the studied compositions were analyzed using X-ray diffraction (XRD) analysis. Figure 1 displays the diffractograms of GeO_2 deposited on a p-Si substrate at different substrate temperatures, recorded with a PANalytical Empyrean XRD model X-ray spectrometer.

According to the literature, Fig. 1 illustrates that all samples exhibit a hexagonal structure. A single prominent peak at approximately 62°, corresponding to the (113) orientation, was observed for GeO_x [18, 20, 21].

In order to look into the impact of substrate temperature, we used the following formula to calculate the structural parameters of the GeO_2 thin films. Bragg's equation (Eq. 1) is used to estimate the interplanar distance.

$$2d\,\mathrm{Sin}\theta = n\lambda \tag{1}$$

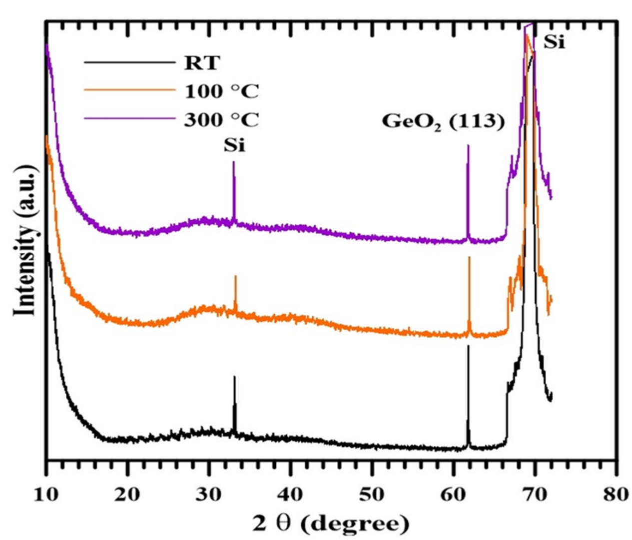

Fig. 1 XRD plot of GeO_2 thin films produced on silicon with the variation of substrate temperatures

where d is interplanar spacing, n is the order of diffraction, θ is the incident angle, and λ is the wavelength.

The determination of nanocrystal crystallite size was performed through the application of Scherer's formula (Eq. 2):

$$D = \frac{k\lambda}{\beta cos\theta_B} \tag{2}$$

where $k = 0.94$ (shape factor), $\lambda = 1.5406$ Å, $\beta =$ full width at half maxima (FWHM) in radian, and θ_B is the Bragg angle.

The lattice constants (a and c) of the GeO_2 phase were calculated according to Eq. 3 for the hexagonal structure:

$$\frac{1}{d_{\mathrm{hkl}}^2} = \frac{4\left(h^2 + hk + l^2\right)}{3a^2} + \frac{l^2}{c^2} \tag{3}$$

and:

$$\frac{c}{a} = \sqrt{\frac{8}{3}} = 1.63 \tag{4}$$

where (hkl) is the Miller indices.

We calculated the strain (ε) in the films by employing the following formula (Eq. 5):

$$\varepsilon = \beta\, cos\theta / 4 \tag{5}$$

Table 1 presents the structural parameters, including grain size (D), FWHM (β), and strain (ε), for all the films.

It is obvious that with increasing substrate temperature, the intensity of the (113) peak increases and sharpens, and the grain size increases. The FWHM and the strain decrease as the substrate temperature increases. In accordance with the research conducted by Yang and Zhang [22], there is an increase in peak intensity and a decrease in the full width at half maximum of the (113) peak. Consequently, it can be inferred that higher substrate temperatures during the deposition process promote the growth of thin films with improved crystallinity and reduced structural disorder. Added to that, the decrease in the strain indicates a decrease in strain is often associated with a reduction in the concentration of lattice imperfections as the substrate temperature increases. As a result, increasing substrate temperature during deposition can lead to improved structural quality and reduced lattice imperfections in thin films or crystals. The improved crystallinity can have significant implications for the performance and properties of the thin films, making them more suitable for various applications in electronics, optics, and other fields where high-quality materials are required.

Table 1 Structural properties of GeO_2 under varying substrate temperatures

Samples	RT	100 °C	300 °C
2θ (°)	61.79	61.94	61.77
Peak intensity	25.622	27.710	42.013
FWHM (°)	0.0812	0.0726	0.0774
$\boldsymbol{D}$ (nm)	114.56	128.29	120.55
$\boldsymbol{\varepsilon}$ ($\times 10^{-4}$)	3.024	3.152	2.874
$\boldsymbol{d}$ (Å)	1.499	1.496	1.499
$\boldsymbol{a}$ (Å)	4.075	4.067	4.076
$\boldsymbol{c}$ (Å)	6.643	6.629	6.645

Scanning electron microscope (SEM)

SEM measurements were conducted on the sample's cross-section, specifically to measure the thickness. The films were found to have thicknesses of approximately 240.60 nm, 166.71 nm, and 148.65 nm, respectively. Figure 2a–c presents SEM analyses.

As seen from the SEM cross-sections, as the substrate temperature rises, the layer thickness reduces. There might be several explanations for the reduction in thickness as substrate temperature rises. At the high deposition temperatures of the films, the adsorbed atoms diffuse to fill the space between the crystals. Accordingly, smoother and denser films are obtained. Apart from that, the high substrate temperature is thought to promote the desorption of adsorbed atoms with lower kinetic energies [23–25].

Raman study

A Raman spectroscopy investigation of GeO_2 was done to establish the vibration mode in the material. It is an effective method for studying GeO_2 materials. Raman scattering in GeO_2 layers may be used to examine strain relaxation. The positions of Raman peaks are associated with phonon–phonon interactions, which vary depending on the material. According to Raman scattering conditions, both Ge–O and Si phonon modes can be detected [26].

Figure 3 shows typical Raman spectra obtained from three GeO_2 samples at room temperature while using a low excitation strength to avoid laser-induced heating. The laser excitation is 532 nm. In each of the samples, the prominent phonon bands can be attributed to the GeO_2-like and Si-like components. Specifically, these bands are detected in the ranges of 50 to 450 cm^{-1} and 480 to 1000 cm^{-1}, respectively. All samples show two peaks at 960 cm^{-1} and 520 cm^{-1} that are associated with transversal optical (TO) and first-order optical characteristic phonon modes of the Si substrate, respectively [27]. The broad spectral peak observed at approximately 100 cm^{-1} can be related to the TA-like phonon mode of Ge nanocrystals, a phenomenon typically forbidden in one-phonon Raman scattering. However, because of the disruption in translational symmetry, this limitation on first-order scattering is lifted [28]. The two 170 and 270 cm^{-1} peaks correspond to A_1 Raman active mode b (O–Ge–O). A peak

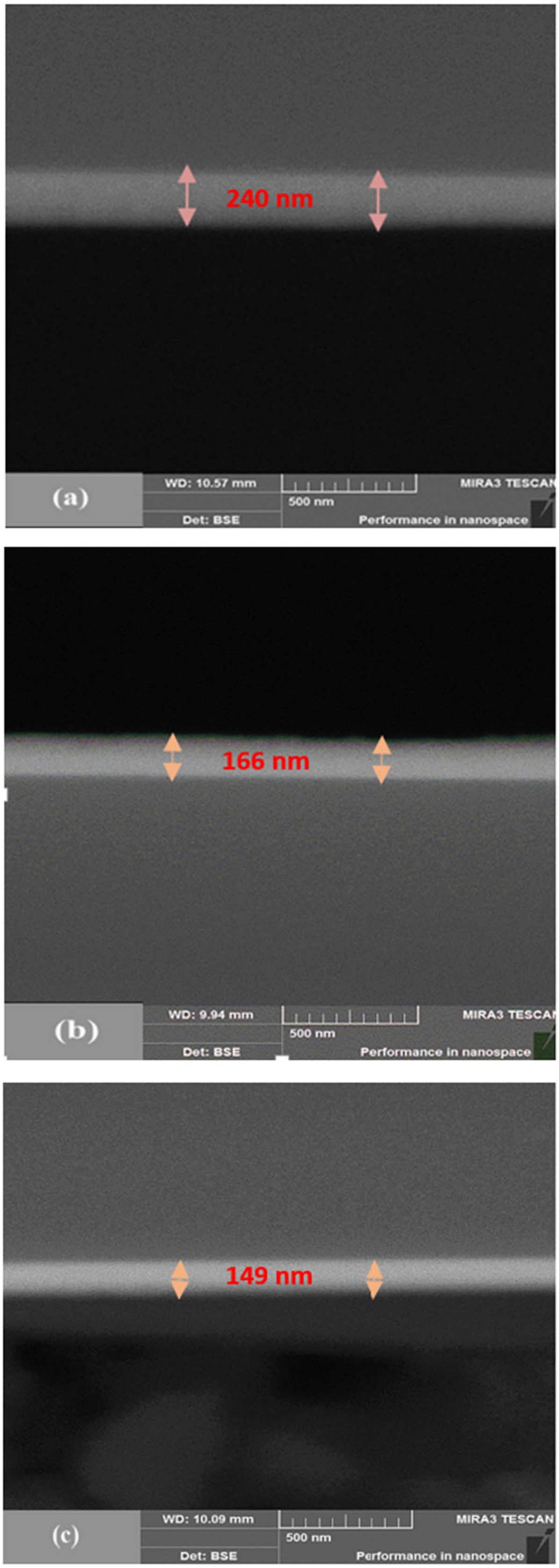

Fig. 2 **a**–**c** SEM cross-sectional analysis of GeO_x films as a function of substrate temperature

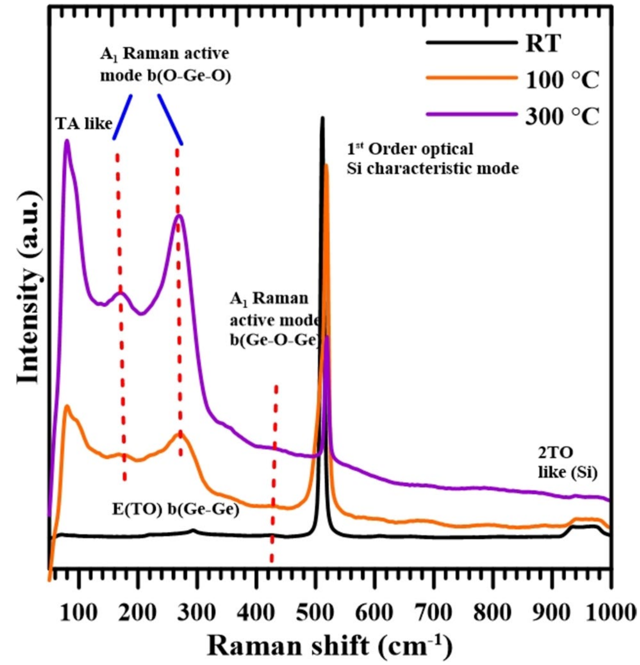

Fig. 3 Raman spectra of GeO_2 with substrate temperature variation

at 425 cm^{-1} is presented in the spectra, which correspond to A_1 Raman active mode b (Ge–O-Ge). Another peak is detected only in the sample spectrum obtained at an ambient temperature of 301 cm^{-1}, which is associated with the E transversal optical (TO) b (Ge–Ge) mode [29]. Based on this spectrum, as the substrate temperature rises, there is a rise in peak intensity with a drop in the full width at half maximum (FWHM), indicating an extended lifespan for the phonons. This demonstrates that the higher the substrate temperature, the more ordered the structure will be, and the defects will be less observable [30].

Optical spectrophotometer

The optical characteristics of GeO_2 films, with varying substrate temperatures, were assessed employing a UV–Vis-NIR spectrophotometer with an integrating sphere, Varian Cary 5000 model. In this analysis, PTFE was used as the reference disk. Figure 4 displays the total reflectance spectrum of GeO_x on a p-Si substrate at various substrate temperatures within the wavelength interval of 200–1200 nm. As seen in this diagram, the interference fringes vanish with the elevation of the temperature of the substrate. The total reflection is affected by an increase in substrate temperature. It can be said that this variation is connected to particle size changes.

Figure 5 shows the diffuse reflectance spectrum of GeO_2 layers at varying substrate temperatures. The measurement of diffuse reflection is crucial for our determination of the optical band gap.

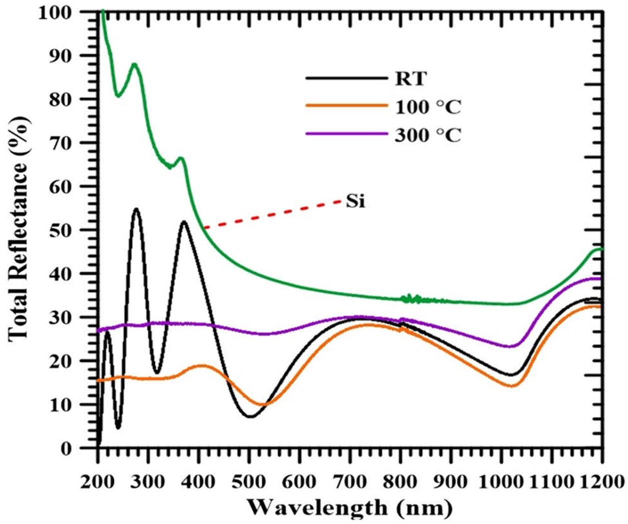

Fig. 4 Total reflectance spectra of GeO_2 films with different substrate temperatures

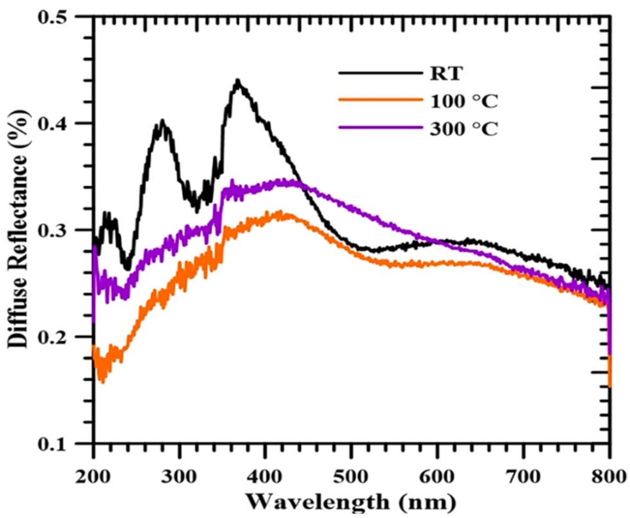

Fig. 5 Diffuse reflectance spectra of GeO_2 films with different substrate temperature

The Kubelka–Munk theory provides the means to determine the energy gap of films deposited on nontransparent substrates, with the sample's diffuse reflectance being connected to the Kubelka–Munk function denoted as $F(R)$. The calculation of diffuse reflectance data was carried out utilizing the Kubelka–Munk function through the following relationship [31]:

$$F(R) = \frac{(1-R)^2}{2R} = \frac{K}{s} \quad (6)$$

This equation relates the diffuse reflectance of the sample (R) to the Kubelka–Munk function ($F(R)$), where K represents the absorption coefficient and s represents the scattering coefficient.

As depicted in Fig. 6, the absorption edge shifts with variations in the substrate temperature. This situation can be related to the change in the energy band gap. Tauc's equation is employed to establish a connection between the absorption coefficient of a direct band gap semiconductor [32, 33].

$$\alpha h\nu = A\left(h\nu - E_g\right)^n \quad (7)$$

This equation relates the linear absorption coefficient (α) of the material to photon energy (hν) through a proportionality constant (A) and a constant factor (n), which depends on the type of optical transition ($n = 1/2$ indicates direct allowed transition).

The Kubelka–Munk function exhibits a direct proportionality to the absorption coefficient.

$$\alpha = \frac{F(R)}{t} \quad (8)$$

where t is the thickness of the film [34]. The energy band gap of the films can be determined by graphing the square of the Kubelka–Munk function against energy. Based on this analysis, it was found that all the films investigated in our research exhibit a direct energy gap. The energy band gap of the films in Fig. 7 is obtained from the intercept of the linear section of the curve with the x-axis.

The associated values of E_g have been provided in Table 2.

It is observed that as substrate temperature rises, the band gap energy decreases from 4.30 to 3.20 eV. This drop in band gap energy can be attributed to changes in film density and grain size in the examined films [35].

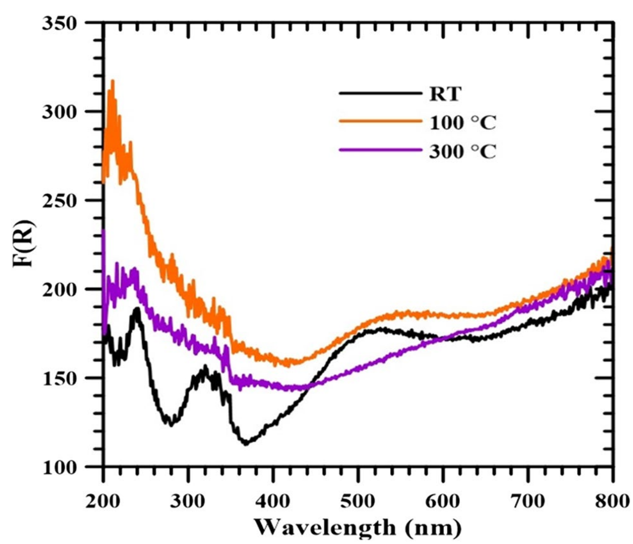

Fig. 6 $F(R)$ versus wavelength

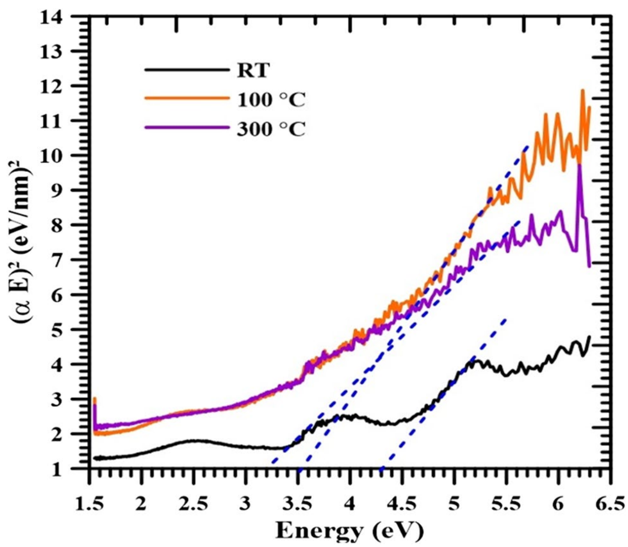

Fig. 7 $(\alpha E)^2$ spectra of GeO_2 films with different substrate temperatures

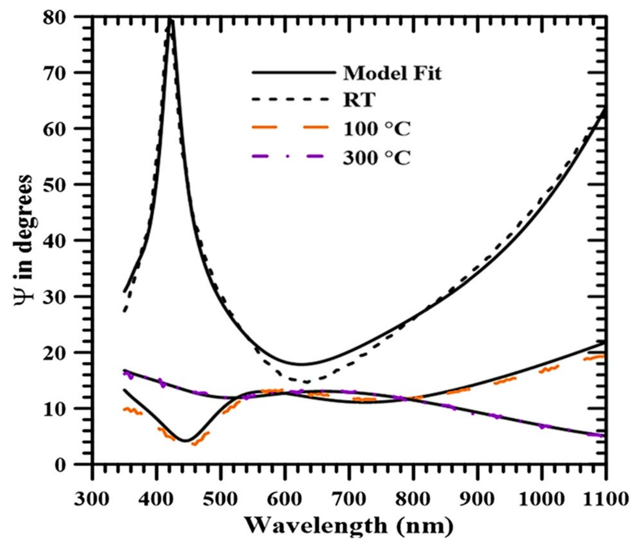

Fig. 8 The spectral dependence of ψ with substrate temperature variation

Table 2 The energy band gap of GeO_x films with different substrate temperatures

Samples	Thickness (nm)	Energy band gap (eV)
RT	240.60	4.30
100 °C	166.71	3.54
300 °C	148.65	3.20

On the other hand, in semiconductors, the thermal energy of the electron increases with increasing substrate temperature. Therefore, electrons require less energy to break the covalent bond and jump to the conduction band. The decrease in binding energy also reduces the distance between the conduction and valence bands [36].

Spectroscopic ellipsometry

The OPT-S9000 Ellipsometer was utilized to do a more detailed optical study using the spectroscopic ellipsometry method. Ellipsometry was employed for the assessment of the films' refractive index, extinction coefficient, and dielectric constant [37, 38]. In this analysis, measurements were conducted within the wavelength spectrum of 350–1100 nm, utilizing a 5 nm increment and an incident angle of 65°. The Cauchy model was employed for the computation of the measurements [39]. Figure 8 illustrates the theoretical and experimental representative spectroscopic Ψ measurements for all sample data across various wavelengths.

Figure 9 displays the theoretical and experimental spectroscopic Δ measurements for all samples as a function of wavelength. It is evident from both plots that the fit is highly accurate, with mean squared error (MSE) values falling within the range of 5–14.

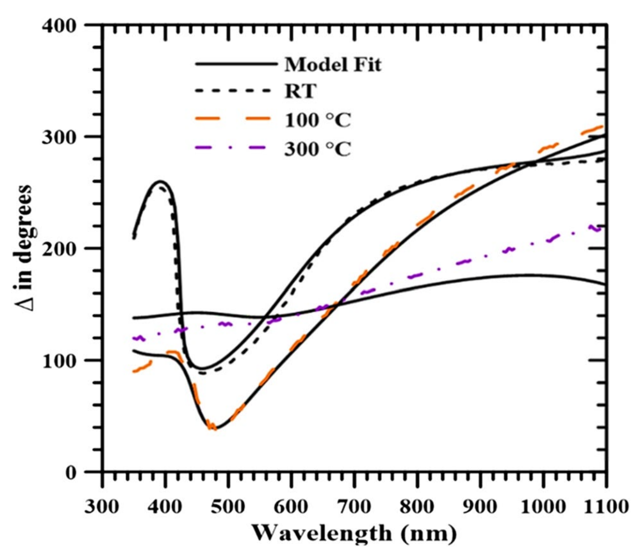

Fig. 9 The spectral dependence of Δ with substrate temperature variation

The refractive indices of GeO_2 films were extracted by examining the Ψ spectra, focusing on the point where the theoretical model and experimental data exhibited the strongest correlation. The graph in Fig. 10 indicates the change in refractive index of GeO_2 films. that were fabricated using various substrate temperatures and on a silicon substrate.

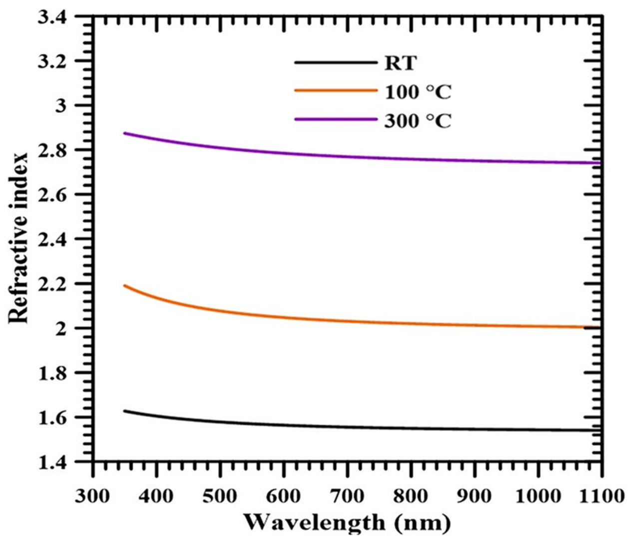

Fig. 10 The variation in the refractive index (n) with respect to the wavelength in GeO_2 films

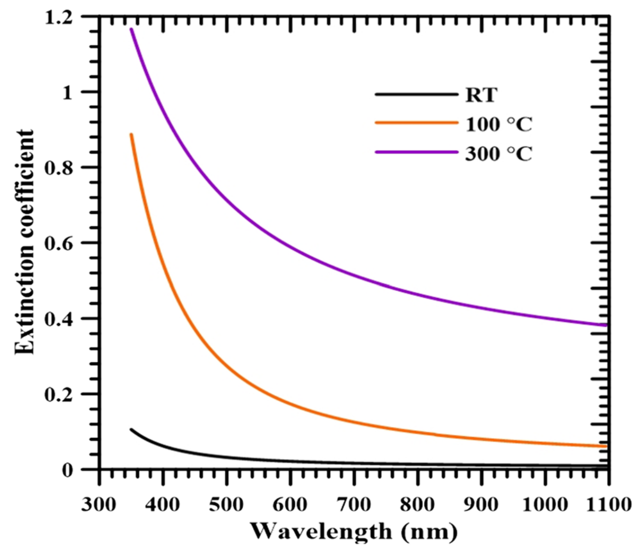

Fig. 11 The relationship between the extinction coefficient and the wavelength in GeO_2 films

The refractive index is directly related to the internal structure of the film under consideration. As can be observed in Fig. 10, significant changes in the refractive index were observed as the substrate temperature changed. The refractive index of the films rises concurrently with a decrease in the optical band gap, as illustrated in Table 2. It is evident that the rise in substrate temperature leads to an increase in the refractive index of the films, likely attributed to the enhanced film packing density and crystallinity. The relationship between the refractive index and film packing density can be readily elucidated through the established Lorentz-Lorenz relation [40]. According to the XRD data, grain size rises with increasing substrate temperature, and sample packing density is inversely related to grain size. As a result, the packing density of the films gradually decreases with rising substrate temperature: a behavior that gives clear proof for the association between the packing density and the refractive index of the GeO_2 films. The results of this study confirm our prior argument that film densification might be one of the reasons leading to the decrease in band gap with rising substrate temperature.

The graph in Fig. 11 illustrates the variation of the extinction coefficient of GeO_2 films fabricated using various substrate temperatures and a silicon substrate. It can be asserted that with the elevation of substrate temperature, there is a corresponding increase in the extinction coefficient.

Furthermore, the complex dielectric constant of a solid, representing the optical properties of thin films, is expressed as

$$\widehat{\varepsilon}(\lambda) = \varepsilon_1(\lambda) + i\varepsilon_2(\lambda) \tag{9}$$

In this context, $\varepsilon_1(\lambda)$ and $\varepsilon_2(\lambda)$ are associated with $n(\lambda)$ and $k(\lambda)$ as follows:

$$\varepsilon_1(\lambda) = n^2(\lambda) - k^2(\lambda) \tag{10}$$

$$\varepsilon_2(\lambda) = 2n(\lambda)k(\lambda) \tag{11}$$

The real part of the dielectric function was calculated, and a graphical representation of $\varepsilon_1(\lambda)$ depending on wavelength is presented in Fig. 12.

The real part of the dielectric constant increased as the elevation of substrate temperature. The imaginary

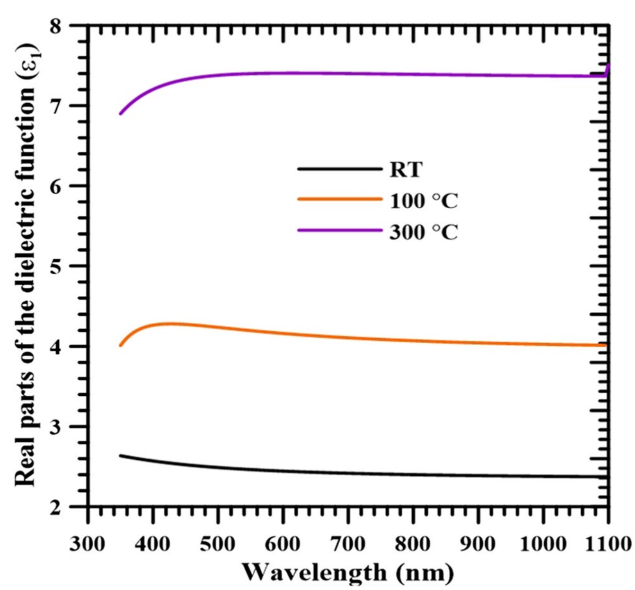

Fig. 12 Real parts (ε_1) of the dielectric function as a function of the wavelength

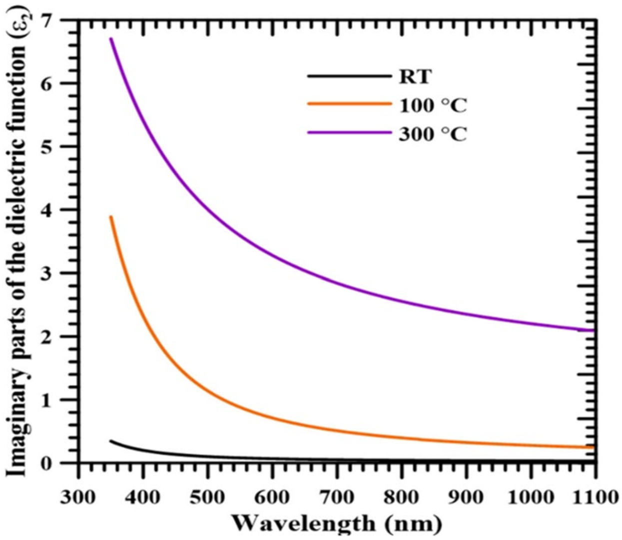

Fig. 13 Imaginary parts of the dielectric function depending on the wavelength

component of the dielectric function $\varepsilon_2(\lambda)$ was computed using Eq. 11, and a graphical representation of $\varepsilon_2(\lambda)$ depending on wavelength is displayed in Fig. 13.

As shown in the figure, the value of the dielectric constant is in accordance with the findings in the literature [33]. Both the real and imaginary components exhibit a similar trend, and the real parts are more important than the imaginary parts. The distinction between the real and imaginary components can be attributed to their correlation with the density of states located within the band gap of the films. In addition, it is seen that both ε_1 and ε_2 exhibit a decrease as the wavelength increases within the visible region. Conversely, the real and imaginary components of thin films' values rise as the substrate temperature increases, leading to an elevation in the dielectric constant attributable to the improvement in crystallinity. The enhancement of dielectric properties can also be attributed to the improved film morphology resulting from the increase in substrate temperature.

Conclusions

In this research, GeO_x semiconductor layers were obtained on p-Si substrate at different substrate temperatures by RF sputtering method. The X-ray diffraction (XRD) analysis of the examined compounds indicated that all samples had a hexagonal crystal structure, which was related to the formation of higher-quality films at higher substrate temperatures. The local structure and bonding properties of the produced films were examined with Raman spectroscopy. We determined the film thicknesses using SEM. The optical parameters of the materials under consideration were assessed through the utilization of an optical spectrophotometer and spectroscopic ellipsometer. An observed trend was the rise in the refractive index with increasing substrate temperature. We can conclude from this research that the GeO_x/Si layers have intriguing structural and optical characteristics that make them useful in a variety of applications in the optics and optoelectronic fields. These findings contribute to the understanding of how deposition conditions impact the material's properties, opening up possibilities for designing and engineering novel optical and optoelectronic devices.

Acknowledgements This research is being carried out at Sivas Cumhuriyet University Research and Development Center (CUTAM), Sivas Cumhuriyet University Nanophotonic Application and Research Center and Laboratory of Multifunctional Materials and Applications (LaMMA), Faculty of Sciences of Sfax, University of Sfax, Tunisia. The authors would like to thank Dr. Sevda Sartaş of Atatürk University in Turkey for her assistance with the XRD characterization.

Data availability Not applicable.

Declarations

Consent to participate Not applicable.

Consent for publication Not applicable.

Competing interests The authors declare no competing interests.

References

1. Rathore, M.S., Vinod, A., Angalakurthi, R., Pathak, A.P., Singh, F., Thatikonda, S.K., Nelamarri, S.R.: Ion beam modification of structural and optical properties of GeO_2 thin films deposited at various substrate temperatures using pulsed laser deposition. Appl. Phys. A **123**, 708 (2017)
2. Rahman, M., Newaz, M.A., Mondal, B.K., Kuddus, A., Karim, M.A., Rashid, M.M., Rubel, M.H.K., Hossain, J.: Unraveling the electrical properties of solution-processed copper iodide thin films for CuI/n-Si solar cells. Mater. Res. Bull. **118**, 110518 (2019)
3. Rahman, Md.F., Hossain, J., Kuddus, A., Tabassum, S., Rubel, M.H.K., Shirai, H., Ismail, A.B.M.: A novel synthesis and characterization of transparent CdS thin films for CdTe/CdS solar cells. Appl. Phys. A **126**(2), 145 (2020)
4. Rashid, Md.A., Mondal, B.K., Rubel, M.H.K., Rahman, Md.M., Mefford, O.T., Hossain, J.: Synthesis of self-assembled randomly oriented VO_2 nanowires on a glass substrate by a spin coating method. Inorg. Chem. **59**(21), 15707–15716 (2020)
5. Rathore, M.S., Vinod, A., Angalakurthi, R., Pathak, A.P., Thatikonda, S.K., Nelamarri, S.R.: Role of oxygen pressure on the structural and photoluminescence properties of pulsed laser deposited GeO_2 thin films. Physica B **625**, 413466 (2022)
6. Wu, X.C., Song, W.H., Sun, Y.P., JDu, .J.: Preparation and photoluminescence properties of crystalline GeO_2 nanowires. Chem. Phys. Lett. **349,** 210-214 (2001)
7. Sahnoun, M., Daul, C., Khenata, R., Baltache, H.: Optical properties of germanium dioxide in the rutile structure. Eur. Phys. J. B. **45**, 455–458 (2005)
8. Jiang, Z., Xie, T., Wang, G.Z., Yuan, X.Y.: GeO 2 nanotubes and nanorods synthesized by vapor phase reactions. Mater. Lett. **59**, 416–419 (2005)

9. Wu, W., Zou, X., Li, Q., Liu, B.B., Liu, B., Liu, R., Liu, D., Li, Z., Cui, W., Liu, Z., Li, D., Cui, T., Zou, G.: Simple synthesis and luminescence characteristics of PVP-capped GeO_2 nanoparticles. J. Nanomater. **2011**, 841701 (2010)
10. Margaryan, A., Piliavin, M.A.: Germanate glasses, structure, spectroscopy, and properties. Artech House, Boston (1993)
11. Terakado, N., Tanaka, K.: Photo-induced phenomena in GeO2 glass. J. Non-Cryst. Solids **352**, 3815–3822 (2006)
12. Terakado, N., Tanaka, K.: Photo-ınduced phenomena in sputtered GeO_2 films. J. Non-Cryst. Solids **351**, 54–60 (2005)
13. Zhou, M., Shao, L., Miao, L.: Matrix ısolation ınfrared spectroscopic and density functional theoretical calculations of the GeO_2^- and GeO_4^- anions. J. Phys. Chem. A **106**, 6483–6486 (2002)
14. Su, Y., Liang, X., Li, S., Chen, Y., Zhou, Q., Yin, S., Meng, X., Kong, M.: Self-catalytic VLS growth and optical properties of single-crystalline GeO_2 nanowire arrays. Mater. Lett. **62**, 1010–1013 (2008)
15. Bai, Z.G., Yu, D.P., Zhang, H.Z., Ding, Y., Wang, Y.P., Gai, X.Z., Hang, Q.L., Xio, G.C., Feng, S.Q.: Nano-scale GeO_2 wires synthesized by physical evaporation. Chem. Phys. Lett. **303**, 311–314 (1999)
16. Kim, H.Y., Viswanathamurthi, P., Bhatarai, N., Lee, D.R.: Preparation and morphology of germanium oxide nanofibers. Rev. Adv. Mater. Sci. **5**, 220–223 (2003)
17. Tang, Y.H., Zhang, Y.F., Wang, N., Bello, I., Lee, C.S., Lee, S.T.: Germanium dioxide whiskers synthesized by laser ablation. Appl. Phys. Lett. **74**, 3824–3826 (1999)
18. Ramana, C.V., Carbajal-Franco, G., Vemuri, R.S., Troitskaia, I.B., Gromilov, S.A., Atuchin, V.V.: Optical properties and thermal stability of germanium oxide (GeO_2) nanocrystals with -quartz structure. Mater. Sci. Eng., B **174**, 279–284 (2010)
19. Baghdedi, D., Hopoğlu, H., Sarıtaş, S., Demir, İ, Altuntaş, İ, Abdelmoula, N., Gür, E., Şenadım Tüzemen, E.: Comprehensive growth and characterization study of GeOx/Si. J. Mol. Struct. **1274**, 134398 (2023)
20. Wang, X.Y., Duan, L., Dong, G.F., Wei, P., Wang, W., Wang, L., Qiu, Y.: Synthesis and characterization of nano/microstructured crystalline germanium dioxide with novel morphology. Chinese Sci Bull. **54**(16), 2810–2813 (2009)
21. Lange, T., Njoroge, W., Weis, H., Beckers, M., Wuttig, M.: Physical properties of thin GeO2 films produced by reactive DC magnetron sputtering. Thin Solid Films **365**(1), 82–89 (2000)
22. Yang, S., Zhang, Y.: Effect of substrate temperature on structural and optical properties of radio-frequency magnetron-sputtered $Ce_{0.97}Co_{0.03}O_2$ thin films. Phys. Status Solidi A **219**, 2100630 (2022)
23. Park, H., Alhammadi, S., Reddy, V.R.M., Park, C., Kim, W.K.: Influence of the Al-doped ZnO sputter-deposition temperature on Cu(In, Ga)Se2 solar cell performance. Nanomaterials **12**, 3326 (2022)
24. Kumar, M.: Effect of substrate temperature on surface morphology and optical properties of sputter deposited nanocrystalline nickel oxide films. Mater. Res. Express. **6**, 096404 (2019)
25. Fang, L., Jiang, Y., Zhu, S., Ding, J., Zhang, D., Yin, A., Chen, P.: Substrate temperature dependent properties of sputtered AlN: Er thin film for in-situ luminescence sensing of Al/AlN multilayer coating health. Materials. **11**, 2196 (2018)
26. Zhang, M., Guo, Z., Zhao, L., Yang, S., Zhao, L.: The effect of buffer types on the In0.82Ga0.18As epitaxial layer grown on an InP (100) substrate. Materials. **11**, 975 (2018)
27. Rathore, M.S., Vinod, A., Angalakurthi, R., Pathak, A.P., Singh, F., Kumar, S., Nelamarri, S.R.: Ion beam modification of structural and optical properties of GeO_2 thin films deposited at various substrate temperatures using pulsed laser deposition. Appl. Phys. A **123**, 708 (2017)
28. Mankad, V., Gupta, S.K., Jha, P.K., Ovsyuk, N.N., Kachurin, G.A.: Low-frequency Raman scattering from Si/Ge nanocrystals in different matrixes caused by acoustic phonon quantization. J. Appl. Phys. **112**, 054318 (2012)
29. Lionel Séjourné. Mise au point d'un système d'analyse par spectroscopie raman en cellule blindée application au graphisme nucléaire. Matériaux Métalliques et Céramiques, Conservatoire national Des Arts ET Metiers, Paris (2012)
30. Takci, D.K., Senadim Tuzemen, E., Kara, K., Yılmaz, S., Esen, R., Bağlayan, Ö.: Influence of Al concentration on structural and optical properties of Al-doped ZnO thin films. J. Mater. Sci. Mater. Electron. **25**(5), 2078–2085 (2014)
31. Yakuphanoglu, F.: Electrical characterization and device characterization of ZnO microring shaped films by sol–gel method. J. Alloy. Compd. **507**(1), 184–189 (2010)
32. Mobtakeri, S., Akaltun, Y., Ozer, A., Kılıç, M., Senadım Tüzemen, E., Gür, E.: Gallium oxide films deposition by RF magnetron sputtering; a detailed analysis on the effects of deposition pressure and sputtering power and annealing. Ceram. Int. **47**(2), 1721–1727 (2021)
33. Vasanth Kumar, C.V.R., Mansingh, A.: Effect of target-substrate distance on the growth and properties of rf-sputtered indium tin oxide films. J. Appl. Phys. **65**, 1270 (1989)
34. Lo, Y.S., Choubey, R.K., Yu, W.C., Hsu, W.T., Lan, C.W.: Shallow bath chemical deposition of CdS thin films. Thin Solid Films **520**, 217–223 (2011)
35. Ramana, C.V., Rubio, E.J., Barraza, C.D., Gallardo, A.M., McPeak, S.A., Kotru, S., Grant, J.T.: Chemical bonding, optical constants, and electrical resistivity of sputter deposited gallium oxide thin films. J. Appl. Phys. **115**(4), 043508 (2014)
36. Nunley, T.N., Fernando, N.S., Samarasingha, N., Moya, J.M., Nelson, C.M., Medina, A.A., Zollner, S.: Optical constants of germanium and thermally grown germanium dioxide from 0.5 to 6.6 eV via a multi-sample ellipsometry investigation. J Vac Sci Technol B, Nanotechnol Microelectron: Mater, Process, Meas, Phenom. **34**(6), 061205 (2016)
37. Born, M., Wolf, E.: Principle of optics. Pergamon, New York (1975)
38. Akaltun, Y., Yıldırım, M.A., Ateş, A., Yıldırım, M.: The relationship between refractive index-energy gap and the film thickness effect on the characteristic parameters of CdSe thin films. Optics Communications. **284**, 2307–2311 (2011)
39. Wemple, S.H., DiDomenico, M.: Behavior of the electronic dielectric constant in covalent and ionic materials. Phys. Rev. B **3**, 1338 (1971)
40. Wemple, S.H., DiDomenico, M.: Optical dispersion and the structure of solids. Phys. Rev. Lett. **23**, 1156 (1969)

Filters Clear All

- *Web of Science* Coverage
- Open Access
- Category
- Country / Region
- Language
- Frequency
- Journal Citation Reports

Refine Your Search Results

Journal of the Australian Ceramic Society

Search

Sort By: Relevancy

Search Results

Found 929 results (Page 1) **Share These Results**

Exact Match Found

JOURNAL OF THE AUSTRALIAN CERAMIC SOCIETY

Publisher: **SPRINGER , ONE NEW YORK PLAZA, SUITE 4600 , NEW YORK, United States, NY, 10004**

ISSN / eISSN: **2510-1560 / 2510-1579**

Web of Science Core Collection: **Science Citation Index Expanded**

Additional *Web of Science* Indexes: **Current Contents Engineering, Computing & Technology | Essential Science Indicators**

Share This Journal **View profile page**

** Requires free login.*

Other Possible Matches

AMERICAN CERAMIC SOCIETY BULLETIN

Publisher: **AMER CERAMIC SOC , 600 N CLEVELAND AVE, WESTERVILLE, USA, OH, 43082**

ISSN / eISSN: **0002-7812 / 1945-2705**

Web of Science Core Collection: **Science Citation Index Expanded**

Additional *Web of Science* Indexes: **Current Contents Engineering, Computing & Technology | Current Contents Physical, Chemical & Earth Sciences | Essential Science Indicators**

Share This Journal **View profile page**

** Requires free login.*

5

JOURNAL OF THE CERAMIC SOCIETY OF JAPAN

Publisher: CERAMIC SOC JAPAN-NIPPON SERAMIKKUSU KYOKAI , 22-17, HYAKUNIN-CHO 2-CHOME, SHINJUKU-KU, TOKYO, JAPAN, 169-0073

ISSN / eISSN: **1882-0743 / 1348-6535**

Web of Science Core Collection: **Science Citation Index Expanded**

Additional *Web of Science* Indexes: **Current Contents Engineering, Computing & Technology | Current Contents Physical, Chemical & Earth Sciences | Essential Science Indicators**

Share This Journal View profile page

* *Requires free login.*

JOURNAL OF THE AMERICAN CERAMIC SOCIETY

Publisher: **WILEY , 111 RIVER ST, HOBOKEN, USA, NJ, 07030-5774**

ISSN / eISSN: **0002-7820 / 1551-2916**

Web of Science Core Collection: **Science Citation Index Expanded**

Additional *Web of Science* Indexes: **Current Contents Engineering, Computing & Technology | Current Contents Physical, Chemical & Earth Sciences | Essential Science Indicators**

Share This Journal View profile page

* *Requires free login.*

JOURNAL OF THE EUROPEAN CERAMIC SOCIETY

Publisher: **ELSEVIER SCI LTD , 125 London Wall, London, England, EC2Y 5AS**

ISSN / eISSN: **0955-2219 / 1873-619X**

Web of Science Core Collection: **Science Citation Index Expanded**

Additional *Web of Science* Indexes: **Current Contents Engineering, Computing & Technology | Current Contents Physical, Chemical & Earth Sciences | Essential Science Indicators**

Share This Journal View profile page

* *Requires free login.*

JOURNAL OF THE KOREAN CERAMIC SOCIETY

Publisher: **SPRINGER HEIDELBERG , TIERGARTENSTRASSE 17, HEIDELBERG, GERMANY, D-69121**

ISSN / eISSN: **1229-7801 / 2234-0491**

Web of Science Core Collection: **Science Citation Index Expanded**

Additional *Web of Science* Indexes: **Current Contents Engineering, Computing & Technology | Essential Science Indicators**

Share This Journal View profile page

* *Requires free login.*

TRANSACTIONS OF THE INDIAN CERAMIC SOCIETY

Publisher: **TAYLOR & FRANCIS LTD , 2-4 PARK SQUARE, MILTON PARK, ABINGDON, England, OXON, OX14 4RN**

ISSN / eISSN: **0371-750X / 2165-5456**

Web of Science Core Collection: **Science Citation Index Expanded**

Additional *Web of Science* Indexes: **Essential Science Indicators**

Share This Journal | View profile page

** Requires free login.*

BULLETIN OF THE AUSTRALIAN MATHEMATICAL SOCIETY

Publisher: **CAMBRIDGE UNIV PRESS , EDINBURGH BLDG, SHAFTESBURY RD, CAMBRIDGE, ENGLAND, CB2 8RU**

ISSN / eISSN: **0004-9727 / 1755-1633**

Web of Science Core Collection: **Science Citation Index Expanded**

Additional *Web of Science* Indexes: **Essential Science Indicators**

Share This Journal | View profile page

** Requires free login.*

JOURNAL OF THE AUSTRALIAN MATHEMATICAL SOCIETY

Publisher: **CAMBRIDGE UNIV PRESS , EDINBURGH BLDG, SHAFTESBURY RD, CAMBRIDGE, ENGLAND, CB2 8RU**

ISSN / eISSN: **1446-7887 / 1446-8107**

Web of Science Core Collection: **Science Citation Index Expanded**

Additional *Web of Science* Indexes: **Current Contents Physical, Chemical & Earth Sciences | Essential Science Indicators**

Share This Journal | View profile page

** Requires free login.*

JOURNAL OF ASIAN CERAMIC SOCIETIES

OPEN ACCESS

Publisher: **TAYLOR & FRANCIS LTD , 2-4 PARK SQUARE, MILTON PARK, ABINGDON, England, OXON, OX14 4RN**

ISSN / eISSN: **2187-0764**

Web of Science Core Collection: **Science Citation Index Expanded**

Additional *Web of Science* Indexes: **Current Contents Engineering, Computing & Technology | Current Contents Physical, Chemical & Earth Sciences | Essential Science Indicators**

Share This Journal | View profile page

** Requires free login.*

Items per page: 10 1 – 10 of 929